Int J Clin Exp Med 2015;8(9):14846-14854
www.ijcem.com /ISSN:1940-5901/IJCEM0012403

Original Article

Clinical features and CT/MRI findings of pancreatic acinar cell carcinoma

Li Tian[1,2*], Xiao-Fei Lv[1,2*], Jun-Dong[1,2], Jian Zhou[1,2], Yu Zhang[1,3], Shao-Yan Xi[1,3], Rong Zhang[1,2], Chuan-Miao Xie[1,2]

[1]Collaborative Innovation Center for Cancer Medicine, State Key Laboratory of Oncology in South China, Guangzhou, P. R. China; [2]Department of Imaging Diagnosis Center, Cancer Center, Sun Yat-sen University, Guangzhou, P. R. China; [3]Department of Pathology, Cancer Center, Sun Yat-sen University, Guangzhou, P. R. China. [*]Equal contributors.

Received July 5, 2015; Accepted September 6, 2015; Epub September 15, 2015; Published September 30, 2015

Abstract: To retrospectively review the clinical features and computed tomography (CT) and magnetic resonance imaging (MRI) findings of PAAC so as to improve the accuracy of imaging diagnosis. Seventeen patients with pathologically proven PAAC were enrolled. Their clinical and imaging findings were retrospectively reviewed. The median age of the patients was 56 years (range, 7-74 years). The tumors were located in any part of the pancreas or exophyitc growth, with a median maximal diameter of 68 mm. Thirteen masses presented with ovoid shape. Nine masses had less clear boundaries. Eleven masses showed a variable degree of intratumoral hypodense or necrosis before contrast administration on CT images. Five masses showed hypointense on unenhanced T1 weighted images and hyperintense on T2 weighted images. After contrast administration, the most common enhancement pattern was slight enhancement on arterial phase and persistent enhancement on portal vein phase. Infiltration of tumor into duct and vessels was not common. Five and 2 patients developed hepatic metastasis and local lymphadenopathy, respectively. By the end of the last follow-up, 11 patients survived free of disease. PAAC should be included in the differential diagnosis when a bulky, ovoid, heterogeneous mass, with clear or less clear margins, in the pancreas or peripancreas, with slight and persistent enhancement after contrast administration on CT or MRI images is seen, particularly in elder men.

Keywords: Pancreatic acinar cell carcinoma, clinical feature, computed tomography, magnetic resonance imaging

Introduction

Pancreatic acinar cell carcinoma (PACC) is a rare malignant epithelial neoplasm that exhibits exocrine enzyme production by neoplastic cells and accounts for only 1% of all pancreatic neoplasms, although pancreatic acinar cells represent more than 80% of pancreatic tissue [1-5]. With few exceptions, acinar cell carcinoma occurs during the fifth to seventh decades of life and has a male predominance. PACC usually manifests nonspecific symptoms and signs, such as abdominal pain, weight loss, and abdominal mass; jaundice is less frequent compared with pancreatic ductal adenocarcinoma (DAC). “Schmid’s triad”, a syndrome of subcutaneous fat necrosis, polyarthralgia, and eosinophilia due to increased serum lipase, is typical but very rare in PACC [1].

According to the literature, the prognosis for patients with PACC is poor, and some researchers estimate a median survival rate for PACC patients ranging from 18 to 33 months [6]. However, in recent years, increasing evidence has shown that PACC is characterized by less aggressive growth and has significantly better long-term survival than other pancreatic neoplasms, such as DAC [7]. Therefore, a preoperative correct diagnosis for PACC is very important for therapeutic decision-making and prognosis assessment. Due to its rarity, there are only a few reports on the clinical and imaging appearances, treatment, and outcome of this disease, and all of them are only in the form of case reports or small series [8-15]. In this study, we retrospectively analyzed the clinical features and radiological findings, including computed tomography and magnetic resonance imaging

Table 1. The clinical features of 17 patients with PACCs

Case	Sex	Age	Symptoms	Laboratory test	Treatment	Follow up			
						FD (month)	Recurrence	Metastasis	Result
1	Male	54	AP	Ne	WE+CT	5.6	N	N	CR
2	Male	62	AP	Amylase↑*	WE+CT	3.6	N	N	CR
3	Male	53	AP	AFP↑	WE	11.5	N	N	CR
4	Male	53	AP	Ne	WE+CT	76.2	N	HM	PD
5	Female	13	J	Ne	WE+CT	12.8	N	HM/LM	PD (death)
6	Female	65	AP	Ne	WE	55.8	N	N	CR
7	Male	61	AP	Ne	WE	32.9	N	HM	PD (death)
8	Female	72	AP	Ne	WE	10.2	N	LM	PD (death)
9	Male	40	AP	Ne	WE+CT	54.4	N	N	CR
10	Female	74	AP	Ne	WE+CT	35.6	N	HM	PD (death)
11	Male	59	AP	CA199↑	WE+CT	9.7	N	HM	PD (death)
12	Male	56	NC	Ne	WE+CT	120.1	N	N	CR
13	Male	73	AP	CEA↑	WE+CT	17.0	N	N	CR
14	Male	15	AP	AFP↑	WE+CT	87.5	N	N	CR
15	Male	60	NC	Ne	WE+CT	3.0	N	N	CR
16	Female	7	AP	Amylase↑	WE+CT	20.0	N	N	CR
17	Male	51	NC	Ne	WE	16.4	N	N	CR

Note: AP = abdominal pain; J = jaundice; NC = no complaints; Ne = negative; AFP = Alpha Fetal Protein; CA199 = Carbohydrate Antigen 199; CEA = Carcino Embryonie Antigen; WE = wide excision; CT = chemotherapy; FD = follow-up duration; N = No; HM = hepatic metastasis; LM = lymphatic matastasis; CR = complete response; PD = progressive disease. *: the symbol "↑" denotes elevated tumor marker levels.

(MRI), of a series of pathologically confirmed PACC to improve the recognition of this disease and accuracy of imaging diagnosis.

Material and methods

Patient population

This retrospective study was approved by the institutional review board, and the requirement to obtain informed consent was waived. We performed a comprehensive retrospective review of the medical records of patients with pathologically confirmed PACC treated at our cancer center between January 2005 and January 2015. We reviewed the clinical data, CT and MRI images, as well as follow-up outcome. In total, 17 patients (twelve men and five women; median age, 56 years, range 7-74 years) were enrolled.

Imaging protocol and radiological evaluation

Twelve patients underwent a CT scan, three patients underwent an MR scan, two patients underwent a CT and MR scan sequentially.

The CT scans were performed with a Toshiba Aquilion TM64 (Toshiba Medical Systems, Otawara, Japan) helical CT system. The main imaging parameters were as follows: 5-mm section thickness reconstructions, 25-cm field of view, 120-kV tube voltage, 300-mA current, and a 512 × 512 matrix. An intravenous bolus dose of 100 ml of a non-ionic iodinated contrast agent (iopromide; Ultravist, Bayer Schering Pharma AG, Berlin, Germany) was administered at a rate of 2.5 ml/s.

The MR scans were performed using a 1.5-T system (Signa CV/i; GE Healthcare, Chalfont St Giles, UK). The patients were placed in a supine position, and a body coil was used. T1-weighted, fast spin-echo images in the axial and coronal planes (400-500/10-20), T2-weighted fast spin-echo MR images in the axial and coronal plane and T2-weighted, fat-suppressed, fast spin-echo in the axial and coronal planes (4000-5000/95-110) were obtained prior to injection of contrast material. After an intravenous administration of 0.1 mmol/kg body weight of gadopentetate dimeglumine (Magnevist; Bayer Schering Pharma AG, Berlin, Germany), the axial T1-weighted spin-echo sequence and axial and coronal T1-weighted, fat-suppressed, spin-echo sequences were performed sequentially using the same parameters applied prior to the injection of gadopen-

Table 2. The CT and MRI findings of 17 patients with PACCs

Nu	Site	MD mm	Shape	Margin	Intratumoral hypodense or necrosis on CT	Signal intensity		Enhancement pattern		Intratumoral calcification/ hemorrhage	Bile duct/ Pancreatic duct dilatation	Vascular encase-ment	Metastasis
						T1WI	T2WI	AP	PP				Liver/Lymph gland
1	BTOP	98	Ov	Cl	Y			SE	PE	+/+*	-/-	N	-/-
2	TOP	28	Ov	Lc	N			SE	PE	+/-	-/-	N	-/-
3	BTOP	128	Ov	Cl		Hypo-	Hyper-	SE	PE	-/-	-/-	N	-/-
4	BTOP	110	Ir	Lc		Hypo-	Hyper-	ME	WO	-/+	-/-	Y	+/-
4	BTOP	110	Ir	Lc	Y			ME	WO	-/+	-/-	Y	+/-
5	HOP	52	Ov	Lc	N			IE	WO	-/-	+/+	N	+/+
6	NOP	36	Ir	Lc	Y			SE	PE	-/-	-/+	N	-/-
7	EXO	98	Ov	Cl	Y			IE	WO	-/-	-/-	N	+/-
8	TOP	36	Ov	Cl	N			SE	PE	-/-	-/-	N	-/+
9	TOP	40	Ir	Lc	Y			IE	PE	+/-	-/-	N	-/-
10	EXO	62	Ov	Cl	Y			IE	WO	-/-	-/-	N	+/-
11	HNOP	68	Ov	Lc	Y			ME	WO	-/-	-/-	Y	+/-
12	BTOP	95	Ov	Cl		Hypo-	Hyper-	ME	PE	-/-	-/-	Y	-/-
13	EXO	120	Ov	Lc	Y			ME	WO	+/-	-/-	N	-/-
14	BTOP	110	Ov	Lc	Y			IE	WO	+/-	-/-	N	-/-
15	HNOP	62	Ir	Lc	Y			ME	WO	-/+	-/-	Y	-/-
15	HNOP	62	Ir	Lc		Hypo-	Hyper-	ME	WO	-/+	-/-	Y	-/-
16	EXO	140	Ov	Cl		Hypo-	Hyper-	SE	PE	-/-	-/-	N	-/-
17	HOP	50	Ov	Cl	Y			SE	PE	-/-	-/+	N	-/-

Note: Nu = number; BTOP = the body and tail of the pancreas; TOP = the tail of the pancreas; HOP = the head of the pancreas; NOP = the neck of the pancreas; EXO = exophytic growth; HNOP = the head and neck of the pancreas; MD = maximal diameter; mm = millimeter; Ov = ovoid shape; Ir = irregular shape; Lc = less clear; Cl = clear; Y = yes; T1WI = T1 weighed image; T2WI = T2 weighted image; Hypo- = hyperintense signal; Hyper- = hyperintense signal; AP = arterial phase; PP = portal vein phase; SE = slight enhancement; ME = moderate enhancement; IE = intense enhancement; PE = persistent enhancement; WO = washout; N = no; *: the symbol "+" denotes positive and "-" denotes negative.

tetate dimeglumine. For imaging in the axial plane, a 5-mm section thickness with a 1-mm intersection gap was used. For imaging in the coronal planes, a 6-mm section thickness with a 1-mm intersection gap was used. The image matrix was 512 × 512, and the field of view was 32 cm.

All images were re-evaluated by two radiologists with more than 10 years of experience in radiological evaluation of abdominal tumors and disputes were resolved in consensus. The following findings were analyzed: (1) lesion location (the head, neck, body or tail of the pancreas or exophytic growth), (2) shape and margins, (3) tumor size (largest diameter), (4) density/ signal intensity, (5) enhancement pattern, (6) presence of calcification or hemorrhage, (7) obstruction of pancreatic ductal (>3 mm) or biliary ductal (>8 mm), (8) encasement of adjacent vessels, (9) presence of distant metastatic disease, and (10) presence of peripancreatic lymphadenopathy.

Pathological examination and analysis

All masses were surgically resected within one week after CT/MR examination, and 2 pathologists reviewed the gross appearance of the tumor specimens and hematoxylin and eosin (H&E)-stained sections. Immunohistochemical analysis (IHC) was performed, including anti-alpha 1 antitrypsin (AAT), chymotrypsin, chromogranin A (CgA), synaptophysin (Syn), cytokeratin (CK), vimentin, neuron-specific enolase (NSE), epithelial membrane antigen (EMA), carcinoembryonic antigen (CEA) and insulin. The tissue samples of two masses were stained with diastase digestion periodic acid-Schiff (PAS) to confirm the presence of dPAS-positive granules in the cytoplasm.

Treatment and follow-up

In addition to surgical treatment, some patients received adjuvant chemotherapy.

The follow-up period was estimated from the first day of treatment to the day of death or day of the last examination.

Results

The clinical features of the 17 patients are summarized in **Table 1**. Thirteen patients were older than 50 years (13/17, 76.5%), and there

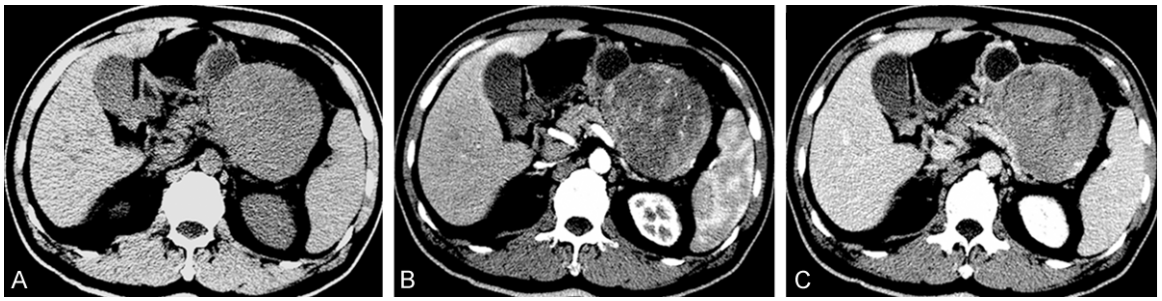

Figure 1. A 54-year-old male with ACC in the body and tail of the pancreas. A. Unenhanced axial CT image showed an ovoid and well-circumscribed mass in the body and tail of the pancreas, with roughly uniform density. B. The mass revealed mild enhancement in the arterial phase when compared to the normal pancreas. C. The mass showed persistent enhancement in the portal vein phase.

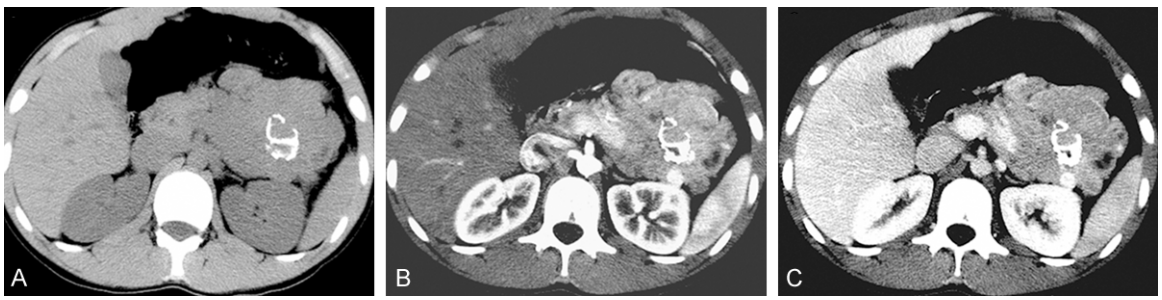

Figure 2. A 15-year-old male with ACC in the body and tail of the pancreas. A. Unenhanced axial CT image showed an ill-circumscribed mass in the body and tail of the pancreas with irregular shape. Strip-shaped calcification was found in it. B. The mass revealed intense enhancement in the arterial phase compared with the pancreatic tissue. C. The contrast agent in the mass washed out in the portal vein phase.

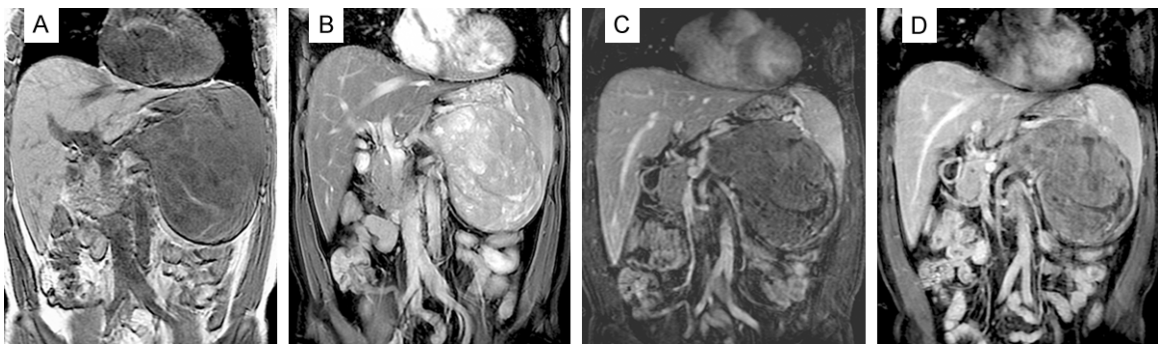

Figure 3. A 53-year-old male with an exophytic ACC. A. Coronal T1 weighed MR image demonstrated an exophytic mass in the left peritoneal cavity, with ovoid shape and clear margin. The mass had a hypointense signal. B. The mass had a heterogeneous, hyperintense signal on the fat-suppressed T2 weighted MR image. C. The mass presented mild enhancement on the fat-suppressed and enhanced T1 weighted MR image in the arterial phase. D. The mass showed persistent enhancement in the portal vein phase.

was an obvious male preponderance in our series (12/17, 70.6%). The majority of patients complained of abdominal pain. Four patients had slightly elevated tumor marker levels, and two had slightly elevated amylase levels. The remaining 11 patients had negative laboratory results. Wide resection of the masses, including resection of pancreatic body and/or tail with or without splenectomy and Whipple procedure, followed by adjuvant chemotherapy, was the main treatment regimen. After 3.0 to 120.1 months of follow-up, 6 patients had metastatic disease, and none developed local recurrence. Five patients died of tumor metastasis, one

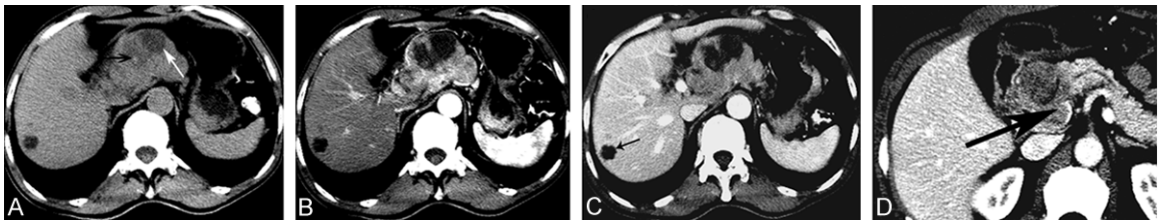

Figure 4. A 59-year-old male with ACC in the head and neck of the pancreas. A. Unenhanced axial CT image showed a mass in the head and neck of the pancreas with ovoid shape and unclear margin. The mass demonstrated a relatively large area of hypodense (white arrow) and patchy hemorrhage (black arrow). B. The mass showed intense enhancement in the arterial phase compared with the pancreatic tissue. C. The contrast agent in the mass washed out in the portal vein phase. A nodule was found in the right and posterior hepatic lobe, which was pathologically confirmed a metastatic lesion of ACC (black arrow). D. The different axial section of the same mass showed the thrombus in the main portal vein (black arrow).

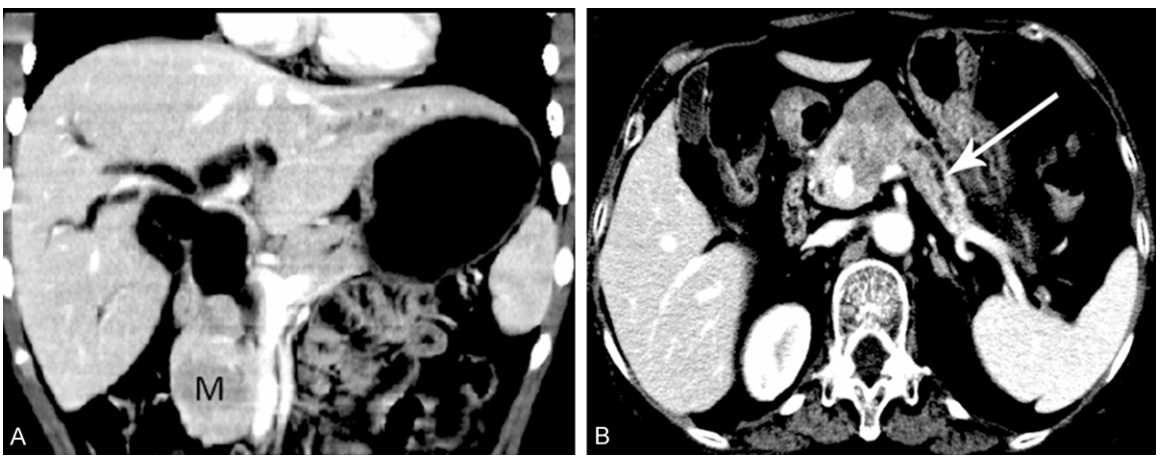

Figure 5. Dilation of bile duct and pancreatic duct of patients with ACC. A. A 13-year-old female with ACC. Enhanced coronal CT image showed that the mass located in the head of the pancreas (M) which infiltrated the common bile duct, resulting in dilation of intrahepatic bile duct and common bile duct. B. A 65-year-old female with ACC. Enhanced axial CT image showed that the mass in the pancreatic neck infiltrated the main pancreatic duct, leading to dilation of the distal pancreatic duct (white arrow).

patient survived with disease, and 11 patients survived free of disease.

The CT and MRI findings of the 17 patients are summarized in **Table 2**. The tumors were located in the body and tail of the pancreas (n=5, **Figures 1**, **2**), the tail of the pancreas (n=3), the head of the pancreas (n=2), the head and neck of the pancreas (n=2), the neck of the pancreas (n=1) and exophytic growth (n=4, **Figure 3**). The maximum diameters of these masses ranged from 28 to 140 mm, with a median maximum diameter of 68 mm. The masses had an ovoid shape (n=13, **Figure 1**) or irregular shape (n=4, **Figure 2**). Eight and 9 masses had clear (**Figure 1**) and less clear margins (**Figure 2**), respectively. Eleven of the fourteen masses detected by CT examination presented with a variable degree of intratumoral hypodensity or necrosis before contrast administration (**Figure 4A**). All of the 5 masses detected by MR examination displayed hypointensity on unenhanced T1-weighted images and hyperintensity on T2-weighted images compared with normal pancreatic parenchyma (**Figure 3A**, **3B**). After contrast administration, the most common enhancement pattern was slight enhancement in the arterial phase and persistent enhancement in the portal vein phase compared with pancreatic parenchyma (7/17, 41.2%) (**Figures 1B**, **1C**, **3C**, **3D**). Then, a pattern of moderate or intense enhancement in the arterial phase and washout in the portal vein phase was observed (4/17, 4/17, 23.5%, respectively, **Figures 2B**, **2C**, **4B**, **4C**). Calcification and hemorrhage were detected in only 5 and 3 masses (**Figures 2A**, **4A**), respectively. Bile duct and pancreatic duct dilatation were observed in 1 and 3 patients,

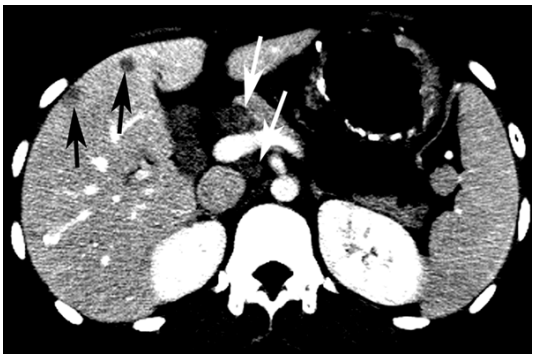

Figure 6. Metastasis of the liver and lymph nodes in the patients with ACC. The same patients as that of **Figure 5A**. The patients developed hepatic and lymphatic metastasis 1 year after operation. Enhanced axial CT image showed the hepatic nodules (black arrows) and the enlarged lymph nodes in the hepatic hilar region and the periphery of vena cava (white arrows).

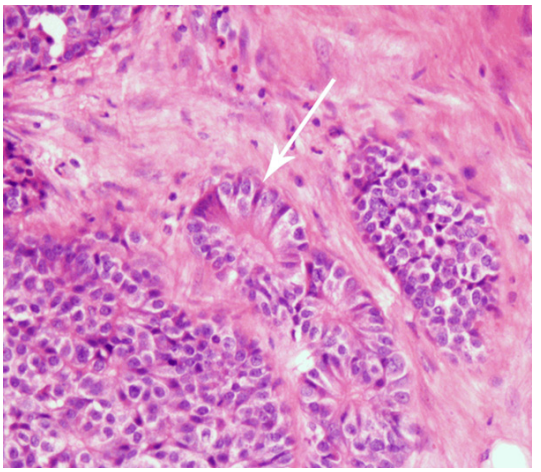

Figure 7. Acinar formation of the neoplastic cells of PACC. The neoplastic cells revealed acinar pattern (white arrow, original magnification ×200).

respectively (**Figure 5A**, **5B**). Four masses had infiltrated the adjacent vessels, including the splenic vein and portal vein (**Figure 4D**). Five patients developed hepatic metastasis, and 2 patients developed local lymphadenopathy (**Figures 4C**, **6**).

The cut surfaces of the masses were greyish white or dark red in appearance, and patchy hemorrhages were observed in 3 cases. Internal areas of necrosis and cystic change were observed in 14 masses. Histologically, the most common patterns observed in PACC are acinar or solid formations (**Figure 7**). The IHC analysis results showed that AAT and chymotrypsin were positive in all masses, whereas CgA and Syn were negative or focally slightly positive. dPAS-positive granules were observed in two masses.

Discussion

The 3 main components of the pancreas are the duct (4%), acinar cells (82%) and islet cells (14%). Although acinar cells occupy most of the normal pancreas, PACC is far less common than DAC, which accounts for more than 90% of total pancreatic neoplasms, and islet cell tumors (ICTs) [16, 17]. PACC, also known as pancreatic acinic cell carcinoma and acinous cell carcinoma [18, 19], was first described by Berner in 1908 [20]. The diagnosis of PACC is based on electron microscopic and immunohistochemical studies [21-23]. PACC cells are characteristically arranged in an acinar formation. Immunohistochemical labeling was strongly positive for trypsin, chymotrypsin, lipase and amylase and negative or only focally positive for chromogranin and synaptophysin.

PACC predominantly affects the elderly, with peak incidence in the seventh decade of life, and male patients outnumber female ones [21-23]. In this study, 76.5% of patients were older than 50 years, and 70.6% of patients were male. Our results were generally consistent with those of previous studies.

Clinically, PACC patients commonly show symptoms related to either a local mass effect or metastases [21, 22, 24]. The most common manifestation in our series was abdominal pain. Only one patient (1/17, 5.9%) presented with jaundice, a relative common sign for DAC patients, which was helpful for the differential diagnosis for both diseases. Interestingly, although PACC can present with “lipase hypersecretion syndrome” [25], which is characterized by fever, arthralgia, skin rash, and fat necrosis due to lipase secretion by the tumor into the blood stream, none of our patients exhibited this clinical manifestation. Additionally, none of our patients had elevated lipase levels. However, slightly elevated AFP, CEA, CA19-9 and amylase levels were observed in a small number of patients, which is concordant with other series [26].

Our results revealed that the masses could affect any part of the pancreas and did not show propensity for the pancreatic head, which has been suggested in previous reports [18,

21, 27]. In contrast, the masses were evenly distributed in the head/neck and body/tail of the pancreas, which was similar to the results of Raman et al [25]. Four masses were located outside the pancreas, and this characteristic can be used to differentiate PACCs from other pancreatic tumors because it is rare in more common pancreatic neoplasms.

The median maximal diameter of the masses was 68 mm, with a maximum value of 140 mm, which was essentially in agreement with previous reports [24, 27, 28]. Moreover, thirteen masses (76.5%) presented with an ovoid shape, and 8 masses (47.1%) had a clear margin. Tatli et al reported the radiological findings of 11 patients with PACC and found that 90.9% of masses presented with an ovoid shape and well-circumscribed margin [18]. Raman et al [25], Butturini et al [1] and Chiou et al [24] obtained similar results. Our results were somewhat different from those of other studies. We speculate that this might be due to our relatively small sample size.

PACC often presents with varying amounts of intratumoral hypodensity on CT images [9-11, 22, 29]. Indeed, 11 of the 14 masses (84.6%) detected by CT revealed different areas of hypodensity, which might be composed of hypovascular neoplastic tissue or a necrotic portion. One possible explanation for the necrotic portion is the digestive effect of the pancreatic enzymes released by neoplastic cells. This feature is helpful for differentiating PACC from DAC, of which the latter commonly appears solid without significant necrosis [24]. All 5 masses detected by MRI exhibited a slightly hypointense signal on T1-weighted images and a hyperintense signal on T2-weighted images compared with pancreatic parenchyma, which was similar to the previous reports [18, 27] and, this finding is not characteristic compared with most malignant tumors.

After contrast administration, most masses had slight or moderate enhancement compared with the normal pancreas in the arterial phase and persistent enhancement in the portal vein phase. This enhancement pattern could be useful for differentiating PACC from DAC and ICT. The degree of enhancement of PACC is usually higher than that of DAC but poorer than that of ICT in the pancreas in the arterial phase [17, 30, 31]. Nevertheless, PACCs may be radiologically indistinguishable from solid-pseudopapillary tumors (SPT) using enhancement pattern. The only valuable feature is that SPTs predominantly affect young women and usually present with intratumoral hemorrhage [32].

Five and 3 masses presented with calcification and hemorrhage, respectively. Calcification within PACC masses has been mentioned in the literature [10, 33], but the occurrence rate is low. Intratumoral hemorrhage of PACCs has been rarely mentioned. Therefore, the presence of calcification and hemorrhage is not significant for the diagnosis of PACCs.

PACCs originate from acinar cells of the pancreas rather than the ductal epithelium; thus, PACCs rarely induce dilatation of the biliary/pancreatic duct [27]. Bile duct and pancreatic duct dilatation was observed in 1 and 3 patients, respectively. This feature is meaningful for differentiating PACC from DAC, which nearly always results in bile duct and pancreatic duct obstruction. In addition, four masses investigated here exhibited infiltration of adjacent vessels, as mentioned in the literature [25, 28], which was a less common feature of PACC.

PACC can develop local and distant metastases, and the most common metastasis locations are liver and lymph gland. In our study, 5 and 2 patients developed hepatic metastasis and local lymphadenopathy, respectively. However, a better prognosis for PACC than DAC can be achieved with complete tumor resection. Twelve patients in our study survived with or without disease during long-term follow-up, and the survival rate was higher than that of previous reports [34, 35]. Unfortunately, 6 patients had a relatively short follow-up period.

In conclusion, PACC usually affects elder men. Typical CT and MR findings of PACC include a large mass with ovoid shape, clear or less clear margin, patchy hypodensity or necrotic component, with slight and persistent enhancement after contrast administration, and lack of ductal dilatation. After surgical removal, the patients recover well.

Disclosure of conflict of interest

None.

Address correspondence to: Drs. Rong Zhang and Chuan-Miao Xie, Department of Imaging Diagnosis Center, Cancer Center, Sun Yat-Sen University, 651 Dongfeng Road, East, Guangzhou 510060, Guangdong, P. R. China. Tel: +86-20-87342125; Fax: +86-20-87342125; E-mail: rongzhangabc@163.com (RZ); Tel: +86-20-87343218; Fax: +86-20-8734-3218; E-mail: chuanmiaoxieabc@163.com (CMX)

References

[1] Butturini G, Pisano M, Scarpa A, D'Onofrio M, Auriemma A and Bassi C. Aggressive approach to acinar cell carcinoma of the pancreas: a single-institution experience and a literature review. Langenbecks Arch Surg 2011; 396: 363-369.

[2] Chen J and Baithun SI. Morphological study of 391 cases of exocrine pancreatic tumours with special reference to the classification of exocrine pancreatic carcinoma. J Pathol 1985; 146: 17-29.

[3] Cubilla AL and Fitzgerald PJ. Morphological patterns of primary nonendocrine human pancreas carcinoma. Cancer Res 1975; 35: 2234-2248.

[4] Cubilla AL and Fitzgerald PJ. Cancer (non-endocrine) of the pancreas. A suggested classification. Monogr Pathol 1980; 21: 82-110.

[5] Morohoshi T, Held G and Kloppel G. Exocrine pancreatic tumours and their histological classification. A study based on 167 autopsy and 97 surgical cases. Histopathology 1983; 7: 645-661.

[6] Wisnoski NC, Townsend CJ, Nealon WH, Freeman JL and Riall TS. 672 patients with acinar cell carcinoma of the pancreas: a population-based comparison to pancreatic adenocarcinoma. Surgery 2008; 144: 141-148.

[7] Sumiyoshi T, Shima Y, Okabayashi T, Kozuki A and Nakamura T. Comparison of pancreatic acinar cell carcinoma and adenocarcinoma using multidetector-row computed tomography. World J Gastroenterol 2013; 19: 5713-5719.

[8] Radin DR, Colletti PM, Forrester DM and Tang WW. Pancreatic acinar cell carcinoma with subcutaneous and intraosseous fat necrosis. Radiology 1986; 158: 67-68.

[9] Ishizaki A, Koito K, Namieno T, Nagakawa T, Murashima Y and Suga T. Acinar cell carcinoma of the pancreas: a rare case of an alpha-fetoprotein-producing cystic tumor. Eur J Radiol 1995; 21: 58-60.

[10] Lim JH, Chung KB, Cho OK and Cho KS. Acinar cell carcinoma of the pancreas. Ultrasonography and computed tomography findings. Clin Imaging 1990; 14: 301-304.

[11] Mustert BR, Stafford-Johnson DB and Francis IR. Appearance of acinar cell carcinoma of the pancreas on dual-phase CT. AJR Am J Roentgenol 1998; 171: 1709.

[12] Sahani D, Prasad SR, Maher M, Warshaw AL, Hahn PF and Saini S. Functioning acinar cell pancreatic carcinoma: diagnosis on mangafodipir trisodium (Mn-DPDP)-enhanced MRI. J Comput Assist Tomogr 2002; 26: 126-128.

[13] Hashimoto M, Matsuda M, Watanabe G, Mori M, Motoi N, Nagai K and Ishibashi M. Acinar cell carcinoma of the pancreas with intraductal growth: report of a case. Pancreas 2003; 26: 306-308.

[14] Chen JD, Wu MS, Tien YW, Kuo KT, Chang MC and Lin JT. Acinar cell carcinoma with hypervascularity. J Gastroenterol Hepatol 2001; 16: 107-111.

[15] Lingg G, Nebel G, Angelkort A and Kloppel G. Computed tomography in a new type of acinar cell tumour of the pancreas: the solid acinar cell tumour with cystic degeneration. Eur J Radiol 1981; 1: 232-235.

[16] Longnecker DS, Shinozuka H and Dekker A. Focal acinar cell dysplasia in human pancreas. Cancer-Am Cancer Soc 1980; 45: 534-540.

[17] Mergo PJ, Helmberger TK, Buetow PC, Helmberger RC and Ros PR. Pancreatic neoplasms: MR imaging and pathologic correlation. Radiographics 1997; 17: 281-301.

[18] Tatli S, Mortele KJ, Levy AD, Glickman JN, Ros PR, Banks PA and Silverman SG. CT and MRI features of pure acinar cell carcinoma of the pancreas in adults. AJR Am J Roentgenol 2005; 184: 511-519.

[19] Chaudhary P, Ranjan G, Chaudhary A, Tiwari AK and Arora MP. Acinar cell carcinoma: a rare pancreatic malignancy. Clin Pract 2013; 3: e18.

[20] Matos JM, Schmidt CM, Turrini O, Agaram NP, Niedergethmann M, Saeger HD, Merchant N, Johnson CS, Lillemoe KD and Grutzmann R. Pancreatic acinar cell carcinoma: a multi-institutional study. J Gastrointest Surg 2009; 13: 1495-1502.

[21] Holen KD, Klimstra DS, Hummer A, Gonen M, Conlon K, Brennan M and Saltz LB. Clinical characteristics and outcomes from an institutional series of acinar cell carcinoma of the pancreas and related tumors. J Clin Oncol 2002; 20: 4673-4678.

[22] Klimstra DS, Heffess CS, Oertel JE and Rosai J. Acinar cell carcinoma of the pancreas. A clinicopathologic study of 28 cases. Am J Surg Pathol 1992; 16: 815-837.

[23] Morohoshi T, Kanda M, Horie A, Chott A, Dreyer T, Kloppel G and Heitz PU. Immunocytochemical markers of uncommon pancreatic tumors. Acinar cell carcinoma, pancreatoblastoma, and solid cystic (papillary-cystic) tumor. Cancer-Am Cancer Soc 1987; 59: 739-747.

[24] Chiou YY, Chiang JH, Hwang JI, Yen CH, Tsay SH and Chang CY. Acinar cell carcinoma of the pancreas: clinical and computed tomography manifestations. J Comput Assist Tomogr 2004; 28: 180-186.
[25] Raman SP, Hruban RH, Cameron JL, Wolfgang CL, Kawamoto S and Fishman EK. Acinar cell carcinoma of the pancreas: computed tomography features--a study of 15 patients. Abdom Imaging 2013; 38: 137-143.
[26] Khalili M, Wax BN, Reed WP, Schuss A, Drexler S, Weston SR and Katz DS. Radiology-pathology conference. Acinar cell carcinoma of the pancreas. Clin Imaging 2006; 30: 343-346.
[27] Hsu MY, Pan KT, Chu SY, Hung CF, Wu RC and Tseng JH. CT and MRI features of acinar cell carcinoma of the pancreas with pathological correlations. Clin Radiol 2010; 65: 223-229.
[28] Hu S, Hu S, Wang M, Wu Z and Miao F. Clinical and CT imaging features of pancreatic acinar cell carcinoma. Radiol Med 2013; 118: 723-731.
[29] Mizuta Y, Isomoto H, Futuki Y, Ehara N, Takeshima F, Omagari K, Murase K, Yakata Y, Senjyu M, Masuda J, Ikuno N, Haraguchi M, Iwasaki K, Shimokawa I and Kohno S. Acinar cell carcinoma of the pancreas associated with hypoglycemia: involvement of “big” insulin-like growth factor-II. J Gastroenterol 1998; 33: 761-765.
[30] Buetow PC, Parrino TV, Buck JL, Pantongrag-Brown L, Ros PR, Dachman AH and Cruess DF. Islet cell tumors of the pancreas: pathologic-imaging correlation among size, necrosis and cysts, calcification, malignant behavior, and functional status. AJR Am J Roentgenol 1995; 165: 1175-1179.
[31] Eelkema EA, Stephens DH, Ward EM and Sheedy PN. CT features of nonfunctioning islet cell carcinoma. AJR Am J Roentgenol 1984; 143: 943-948.
[32] Ohtomo K, Furui S, Onoue M, Okada Y, Kusano S, Shiga J and Suda K. Solid and papillary epithelial neoplasm of the pancreas: MR imaging and pathologic correlation. Radiology 1992; 184: 567-570.
[33] Itoh T, Kishi K, Tojo M, Kitajima N, Kinoshita Y, Inatome T, Fukuzaki H, Nishiyama N, Tachibana H, Takahashi H and Et A. Acinar cell carcinoma of the pancreas with elevated serum alpha-fetoprotein levels: a case report and a review of 28 cases reported in Japan. Gastroenterol Jpn 1992; 27: 785-791.
[34] Kitagami H, Kondo S, Hirano S, Kawakami H, Egawa S and Tanaka M. Acinar cell carcinoma of the pancreas: clinical analysis of 115 patients from Pancreatic Cancer Registry of Japan Pancreas Society. Pancreas 2007; 35: 42-46.
[35] Shah S and Mortele KJ. Uncommon solid pancreatic neoplasms: ultrasound, computed tomography, and magnetic resonance imaging features. Semin Ultrasound CT MR 2007; 28: 357-370.